https://dx.doi.org/10.21577/0103-5053.20210158

J. Braz. Chem. Soc., Vol. 33, No. 4, 406-412, 2022

Short Report

Atomic Absorption Spectrometry as an Alternative to Determine the Presence of Gold Nanoparticles on or in Silica Matrix

Cristian J. Giertyas,[a] Victor E. S. Silva,[a] Maria J. de Oliveira,[b] Emerson S. Freire,[b] Josué C. C. Santos,[b] Rusiene M. de Almeida,[a] Mario R. Meneghetti[a] and Janaína H. Bortoluzzi[*,a]

[a]Grupo de Catálise e Reatividade Química, Instituto de Química e Biotecnologia (GCaR), Universidade Federal de Alagoas, Avenida Lourival de Melo Mota s/n, Campus A.C. Simões, 57072-900 Maceió-AL, Brazil

[b]Laboratório de Instrumentação e Desenvolvimento em Química Analítica (LINQA), Universidade Federal de Alagoas, Avenida Lourival de Melo Mota s/n, Campus A.C. Simões, 57072-900 Maceió-AL, Brazil

Two different gold-silica-based nanomaterials were prepared: (*i*) silica-supported gold nanoparticles (AuNP/SiO_2); and (*ii*) gold-silica core-shell nanoparticles (AuNP@SiO_2). Three strategies for sample treatment (S), consisting in acid treatments, were employed: (S1) HNO_3; (S2) HNO_3 + HCl; and (S3) HF + HNO_3 + HCl, applying microwave oven digestion for S2 and S3. From three calibration curves, slope, intercept, and linear correlation coefficient were obtained. The accuracy of the methods was evaluated by comparing the gold contents in a sample determined by flame atomic absorption spectrometry (FAAS) and by inductively coupled plasma atomic emission spectrometry (ICP-OES). Finally, the amount of gold for all samples was determined by FAAS. UV-Vis spectroscopy and transmission electron microscopy (TEM) were used to compare the material before and after sample treatment. By comparison, the application of S2 and S3 allowed the presence of gold on or in the silica matrix to be determined and the amount quantified.

Keywords: core-shell nanoparticles, supported metal nanoparticles, characterization of nanoparticles, gold, silica, flame atomic absorption spectrometry, sample preparation

Introduction

Metallic nanoparticles, along with their salts and oxide derivatives, have several applications in important areas, including catalysis and biomedicine.[1-3] In general, these metal-based nanoparticles are not employed in their isolated pure form but are associated with other organic or inorganic components to provide them with stability or a particular property or potential use. However, materials containing different components are more complex in terms of determining and quantifying their components.[4]

Gold nanoparticles (AuNPs) have a wide variety of applications, mostly due to the unique physicochemical properties of metallic gold when it is in these dimensions.[3] It should be noted that, for specific applications, AuNPs are normally supported on or surrounded by an oxide, for example, silica.[5-8] Nanostructured silica presents interesting properties for nanotechnological applications. Silica offers good thermal and chemical stability and biocompatibility, but its surface chemistry is versatile, allowing the functionalization and modulation of its hydrophilicity. Furthermore, in general, nanostructured silica can be easily synthesized in large scale and at low cost. The combination of these attractive characteristics have led to a large variety of silica nanoformulations being proposed and investigated.[9]

All of these nanostructures can be characterized using techniques to determine structural aspects, such as transmission electron microscopy (TEM), scanning tunneling microscopy (STM), scanning electron microscopy (SEM), atomic force microscopy (AFM) and X-ray diffraction (XRD). To determine the chemical composition, energy dispersive X-ray analysis (EDX), X-ray photoelectron spectroscopy (XPS), near-edge X-ray absorption fine structure (NE XAFS) and extended X-ray

*e-mail: janaina.bortoluzzi@iqb.ufal.br
Editors handled this article: Jaísa Fernandes Soares and Pedro H. C. Camargo (Associate)

absorption fine structure (EXAFS) can be employed.[10,11] However, TEM is the technique most commonly used for both structural resolution and chemical mapping.[11-15] This technique allows the silica-supported gold ($AuNP/SiO_2$) and core-shell ($AuNP@SiO_2$) nanostructured systems to be distinguished. On the other hand, for elemental quantification, spectrometric techniques like atomic absorption spectrometry (AAS) (electro-thermal or with flame atomization) and inductively coupled plasma atomic emission spectrometry (ICP-OES), in some cases associated with mass spectrometry, are generally applied. However, when AAS and ICP-OES are used for elemental quantification the sample preparation strategy for a silica-supported metal nanoparticle system it is not necessarily the same as that for an analogous core-shell-like system (e.g., for $AuNP/SiO_2$ and $AuNP@SiO_2$).

In view of this, we evaluated the wet sample preparation processes for $AuNP/SiO_2$ and $AuNP@SiO_2$ systems, adopting different sample preparation strategies based on mixtures of oxidizing (HNO_3) and complexing (HCl and HF) acids, associated with microwave-assisted digestion. Finally, the quantification of the gold content in the different nanostructured systems was performed by flame atomic absorption spectrometry (FAAS).

Experimental

Synthesis of gold-silica-based nanomaterials

The nanoparticles were prepared employing the experimental protocol described by Huh *et al.*[16] and Trewyn *et al.*[17] for $AuNP/SiO_2$, and Arnal *et al.*[18] and Fang *et al.*[19] for $AuNP@SiO_2$, with some adaptations.

Synthesis of silica-supported gold nanoparticles ($AuNP/SiO_2$)

Briefly, in a 1 L Teflon beaker, deionized water (600 mL, obtained from a MilliQ-Plus filtration system, Millipore®, Merck, Darmstadt, Germany), an aqueous solution of NaOH (6.0 mL of 2.0 mol L^{-1}; Dinâmica Química Contemporânea LTDA, São Paulo, Brazil) and hexadecyl trimethylammonium bromide (CTAB) (0.50 g, Acros Organics, Geel, Belgium) were mixed and heated to 50 °C. After 15 min, an aqueous solution of $HAuCl_4.3H_2O$ (12 mL; 1% m/v; Sigma-Aldrich, Missouri, USA) was added and, after homogenizing the solution, tetraethylorthosilicate (TEOS) (3.3 mL; 95%, Sigma-Aldrich, Missouri, USA) was added. After 2 h at 50 °C, the solid was recovered by filtration and washed with deionized water until all excess base had been removed. The solid obtained was dried in an oven at 80 °C for 24 h. Lastly, the solid was calcined at 550 ºC for 4 h with a heating rate of 5 ºC *per* min under ambient atmosphere. At the end of the process a red solid material (0.3 g) was obtained.

Synthesis of gold-silica core-shell nanoparticles ($AuNP@SiO_2$)

Briefly, spherical AuNPs were prepared in a 500-mL reaction flask with the addition of deionized water (280 mL) and an aqueous solution of $HAuCl_4.3H_2O$ (7.5 mL; 1% m/v; Sigma-Aldrich, Missouri, USA). The solution was heated under reflux, when an aqueous solution of sodium citrate (4.2 mL; 3% m/v; Sigma-Aldrich, Missouri, USA) was added. The mixture changed color from yellow to dark red and remained under reflux for a further 30 min. After reaching room temperature, an aqueous solution of polyvinylpyrrolidone (PVP) (1.0 mL; 12.8 g L^{-1}; Sigma-Aldrich, Missouri, USA) was added and the mixture was kept under stirring for 24 h. PVP-stabilized AuNPs were centrifuged at 13500 rpm for 20 min and dispersed in deionized water (55 mL). In the second stage, the colloidal solution of AuNPs was added in a Teflon beaker flask (500 mL) with isopropanol (400 mL; Tedia, Rio de Janeiro, Brazil) and an aqueous solution of ammonium hydroxide (11.0 mL; 28% m/m; Dinâmica Química Contemporânea LTDA, São Paulo, Brazil). After 5 min of mixing, tetraethylorthosilicate (TEOS) (3.3 mL; 95%, Sigma-Aldrich, Missouri, USA) was added dropwise under vigorous stirring, with 1.0 mL being dropped every 5 min into the solution. The solution was covered with aluminum foil and left for 12 h under stirring. The solid formed was collected by centrifugation (13500 rpm *per* 20 min) and then washed with a solution of ethanol/deionized water (1:1; 3 × 20 mL) and dried in an oven at 80 °C for 24 h. Lastly, the solid was calcined at 550 ºC for 4 h with a heating rate of 5 ºC *per* min under ambient atmosphere. At the end of the process a red solid material (1.1 g) was obtained.

Determination of the gold content

The gold content for both nanostructured materials was determined by flame atomization atomic absorption spectrometry (Shimadzu, AA-7000, Kyoto, Japan), using λ = 242.8 nm and a hollow gold cathode lamp. In all three wet sample preparation strategies, 50 mg of sample was used. For S1, 10 mL of HNO_3 at 2.0 mol L^{-1} (Merck, Darmstadt, Germany) were added, and the extraction procedure was applied with 30 min of stirring at 600 rpm. The samples were then filtered through cellulose acetate membranes (0.45 μm). For S2 the mineralization procedure was performed in an Ethos One high-pressure closed

microwave (MW) digestion system (Milestone, Sorilose, Italy), equipped with ten (SK-10) rotors, using mixtures of concentrated acids: S2, 2.0 mL 65% (m/m) HNO_3 with 6.0 mL 37% (m/m) HCl (1:3, aqua regia, Merck, Darmstadt, Germany) and 1.0 mL of ultrapure water were added (conductivity < 0.1 μS cm^{-1}). The procedure for S3 was the same as that for S2 but with the addition of 1.0 mL HF 48% (m/m) (Sigma-Aldrich, Missouri, USA) in the place of water. After adding the reagents, the reactors were closed and the heating program (Table 1) was started, according to the conditions recommended by Niemelä *et al.*[20]

Table 1. Digestion program of nanoparticle samples by microwave radiation

Stage	time / min	Power / W	Temperature / ºC
I	15[a]	1000	from RT to 200
II	10[b]	1000	200

[a]Heating ramp time; [b]landing time. RT: room temperature.

Pressurized and closed system digestions were performed in triplicate (n = 3) and, in each procedure, the three reactors contained blank analytical solutions. After the above-mentioned steps (Table 1), the reactors were kept under ventilation for 20 min and then opened and the digested material was cooled to room temperature. The solutions resulting from S2 were filtered (0.45 μm) to separate undissolved silica (SiO_2) and diluted to 25 mL with ultrapure water while those resulting from S3 were additionally treated with 0.50 g of H_3BO_3 (Sigma-Aldrich, Missouri, USA) to eliminate the excess HF present in the reaction medium. The residual acidity of the digests was determined by acid-base titration, using a standardized sodium hydroxide solution (0.0900 mol L^{-1}) and 1.0% (m/v) phenolphthalein as a visual indicator. Calibration curves (1.0 to 25 mg L^{-1} Au content, n = 7) for the gold determination were constructed from the gold precursor salt ($HAuCl_4.3H_2O$, Sigma-Aldrich, Missouri, USA) and used for the nanoparticle synthesis. For each strategy, a calibration curve was prepared considering the composition and final concentration of the acid mixture.

The efficiency of the proposed methodology to determine the gold content of the gold-silica samples was confirmed by comparing the results obtained for a $AuNP/SiO_2$ sample analyzed by ICP-OES carried out at the Analytical Center of the Chemistry Institute of the University of São Paulo. In this procedure a Spectro ICP-OES spectrometer, model Arcos (Kleve, Germany), was used with the following parameters: frequency, 27.12 MHz; power, 1400 W; argon flow rates for plasma, 12 L min^{-1}; auxiliary, 1 L min^{-1}; nebulizer, 0.85 L min^{-1}, sample, 0.85 L min^{-1}, pump rate, 30 rpm; nebulizer, crossbow; emission line, 267.60 nm. For the ICP-OES analysis, the sample was digested in an open system using a mixture of acids (HNO_3, HCl and HF; 0.5:1.5:1, respectively) under heating in a Tecnal digester block, model TE-015-1 (Sao Paulo, Brazil).

Other characterizations

Transmission electron microscopy (TEM) was performed on an FEI Tecnai G2 Spirit TWIN electron microscope (Hillsboro, USA) at an accelerating voltage of 120 kV, and the samples were prepared with the addition of a drop of the gold colloidal solution on a copper grid coated with a porous carbon film. UV-Vis diffuse reflectance spectroscopy (DRS) was performed using a 2600 spectrometer (Shimadzu, Kyoto, Japan) with a solid integrated sphere. The spectra were recorded with a spectral resolution of 8 cm^{-1}, using the diffuse reflectance and absorption mode. The range analyzed was 400-1000 nm and the samples were placed on a support for solids and analyzed in triplicate.

Results and Discussion

To quantify the accessible gold content after the different sample treatments for $AuNP/SiO_2$ and $AuNP@SiO_2$, three calibration curves were prepared, and the analytical parameters related to slope, intercept and the linear correlation coefficient were obtained.

The calibration curves were subjected to analysis of variance (ANOVA, one-way) to evaluate the sensitivity and the analytical blank in the different systems (S1, S2, and S3). It was observed that there was no significant difference between them at the 95% confidence level ($F_{cal} = 0.008 < F_{critical} = 3.5545$). Thus, the 2 mol L^{-1} HNO_3 solution curve was used for the gold quantification in subsequent experiments.

The accuracy of the proposed methods was evaluated by comparing the gold contents in a sample determined by FAAS and by ICP-OES. Using S2, the gold content obtained was 1.71 ± 0.07% (m/m), while the result obtained employing ICP-OES was 1.82 ± 0.10% (m/m). On applying the Student's *t*-test, it was observed that there is no significant difference between the two methods at the 95% confidence level.

After determining the accuracy of the method, it was applied to samples of silica-supported gold nanoparticles ($AuNP/SiO_2$) and the analogous core-shell system ($AuNP@SiO_2$). Table 2 shows the Au concentration for each of the samples, exploring the preparation strategies evaluated. It can be observed that $AuNP/SiO_2$ presented a

Table 2. Gold content determined in nanoparticles by flame atomic absorption spectrometry applying different sample preparation strategies

Sample	Au / (%, m/m)					
	$AuNP/SiO_2$			$AuNP@SiO_2$		
	S1 (± 0.02)	S2 (± 0.03)	S3 (± 0.07)	S1 (± 0.03)	S2 (± 0.04)	S3 (± 0.06)
A1	< LOD	1.56	1.51	< LOD	< LOD	2.65
A2	< LOD	1.56	1.43	< LOD	< LOD	2.74
A3	< LOD	1.62	1.57	< LOD	< LOD	2.75

Sample preparation strategies: S1 = HNO_3 2 mol L^{-1} + 30 min stirring at 600 rpm; S2 = HNO_3 + HCl + microwave; and S3 = HNO_3 + HCl + HF + microwave. The limit of detection (LOD, 3σ) was calculated as 0.10 mg L^{-1}.

lower average gold content (1.5% m/m) when compared to $AuNP@SiO_2$ (2.7% m/m).

On applying S1 (HNO_3) to both nanostructured materials ($AuNP/SiO_2$ and $AuNP@SiO_2$) it was not possible to quantify the ionic gold content (Au^{3+}), which indicates that most of the gold present is in the reduced form (Au^0).

The $AuNP/SiO_2$ and $AuNP@SiO_2$ samples after the S2 treatment were dried and characterized by solid-state UV-Vis spectroscopy and the spectra obtained for the systems evaluated are shown in Figure 1. It can be noted that for the $AuNP@SiO_2$ samples the intensity and profile of the surface plasmon absorption band at around 525 nm (before and after digestion) is similar and characteristic of gold ball-shaped nanoparticles.[11,21] For the $AuNP/SiO_2$ sample after the S2 treatment, the plasmon absorption band is absent, indicating that all gold nanoparticles had been removed from the sample surface. Thus, the UV-Vis spectroscopy results corroborate with the expected data obtained for the sample preparation procedures used.

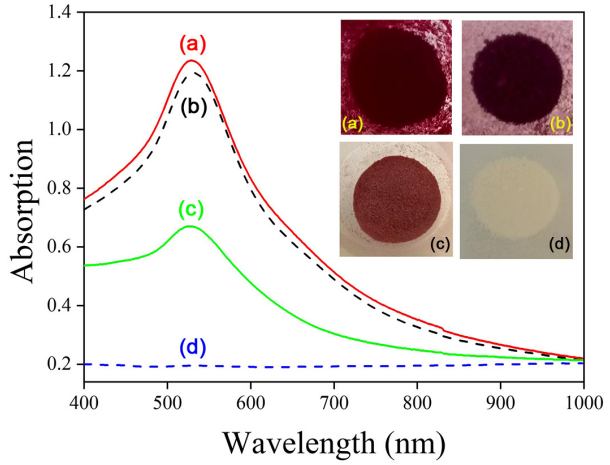

Figure 1. Absorption spectra and corresponding images were obtained by solid-state UV-Vis spectroscopy, for $AuNP@SiO_2$: (a) before and (b) after strategy S2 and $AuNP/SiO_2$: (c) before and (d) after strategy S2. The S2 = HNO_3 + HCl, using MW. The pictures insert to represent the nanoparticles synthesized.

After digestion of the $AuNP@SiO_2$ samples (Figure 1a), it was not possible to detect the gold content using strategy S2 (HNO_3 + HCl + MW), and no visual changes were observed in the aspect of the remaining material (Figure 1b). This result indicates the presence of gold nanoparticles inside the nanomaterial (metal on core) is consistent with a core-shell structure,[21,22] i.e., the gold nanoparticle is covered by a nonporous silica layer, protecting the AuNP core[23] during the S2 treatment. In fact, for S2, on comparing the images of the $AuNP@SiO_2$ samples before and after digestion (Figures 1a and 1b, respectively), it can be observed that the proposed digestion conditions failed to extract the gold nanoparticles present in the silica.

On the other hand, on applying S2, it is possible to detect and quantify the gold content in the $AuNP/SiO_2$ sample, since the AuNPs are supported on the silica particles. After microwave-assisted digestion, a white solid powder was recuperated by filtration (Figure 1d), in contrast to the dark red color of the sample before the S2 treatment (Figure 1c).

Both the $AuNP/SiO_2$ and $AuNP@SiO_2$ samples were entirely solubilized after the S3 digestion (HNO_3 + HCl + HF + MW), leaving the gold available for quantification as Au^{3+}. For the $AuNP/SiO_2$ sample, in which the metal is found only on the surface of the silica, no significant difference in the Au contents was observed on applying the S2 and S3 procedures (Table 1), with 95% confidence applying the Student's paired *t*-test. However, for the $AuNP@SiO_2$ sample, the gold was only quantified after treatment S3, confirming the protection effect of the silica. Therefore, employing the three different sample preparation strategies in a wet system it was possible not only to quantify the amount of gold in the material but also to characterize the structure of the nanomaterial. Finally, Scheme 1 shows a compilation of all the strategies employed in this work.

When the S1 (diluted HNO_3 solution) procedure was applied to the samples ($AuNP/SiO_2$ and $AuNP@SiO_2$) the concentration of Au^{3+} was lower than the limit of detection (LOD), indicating that practically all of the gold content was in its reduced form Au^0 as nanoparticles (Table 1). In

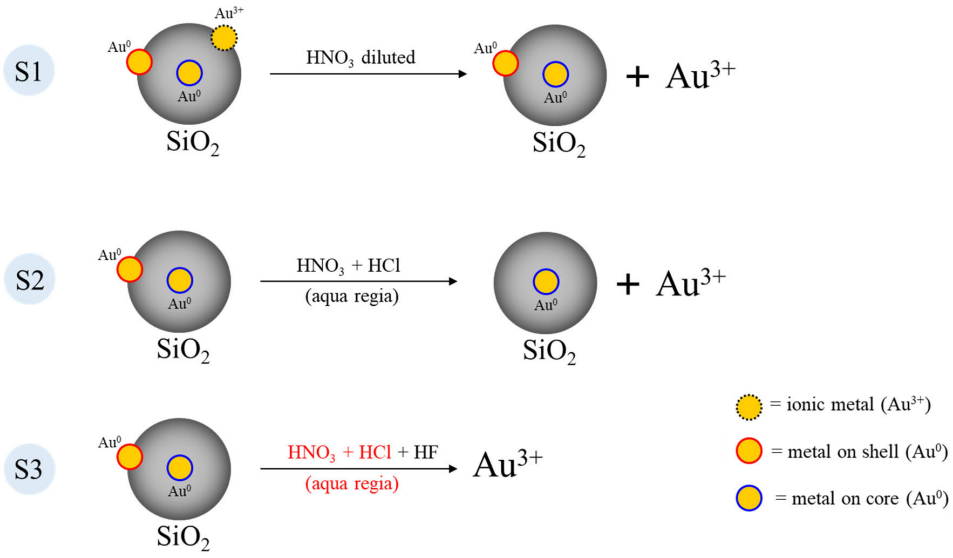

Scheme 1. Summary of strategies and information obtained for the different systems evaluated.

the S2 procedure (aqua regia), all of the gold content was converted to Au^{3+} as the tetrachloroaurate ion ($AuCl_4^-$), according to equation 1. With the application of the S3 procedure, the silica was dissolved due to the presence of HF, according to equation 2, allowing the reaction of aqua regia with the metal core.

$$2Au_{(s)} + 11HCl_{(aq)} + 3HNO_{3(aq)} \rightarrow 2HAuCl_4^-{}_{(aq)} + 3NOCl_{(aq)} + 6H_2O_{(l)} \quad (1)$$

$$SiO_{2(s)} + 6HF_{(aq)} \rightarrow H_2SiF_{6(aq)} + 2H_2O_{(l)} \quad (2)$$

Additionally, the samples were characterized by transmission electron microscopy (TEM) before and after the treatment procedure S2 (Figure 2). After the treatment, the micrographs for $AuNP/SiO_2$ revealed that the gold nanoparticles had been removed. It was also observed that the treatment promoted modification of the morphology of the silica matrix, since there was an increase in surface roughness and the potential formation of larger pores (Figure 2b). On the other hand, on comparing Figures 2c and 2d, it can be seen that the silica-encapsulated gold

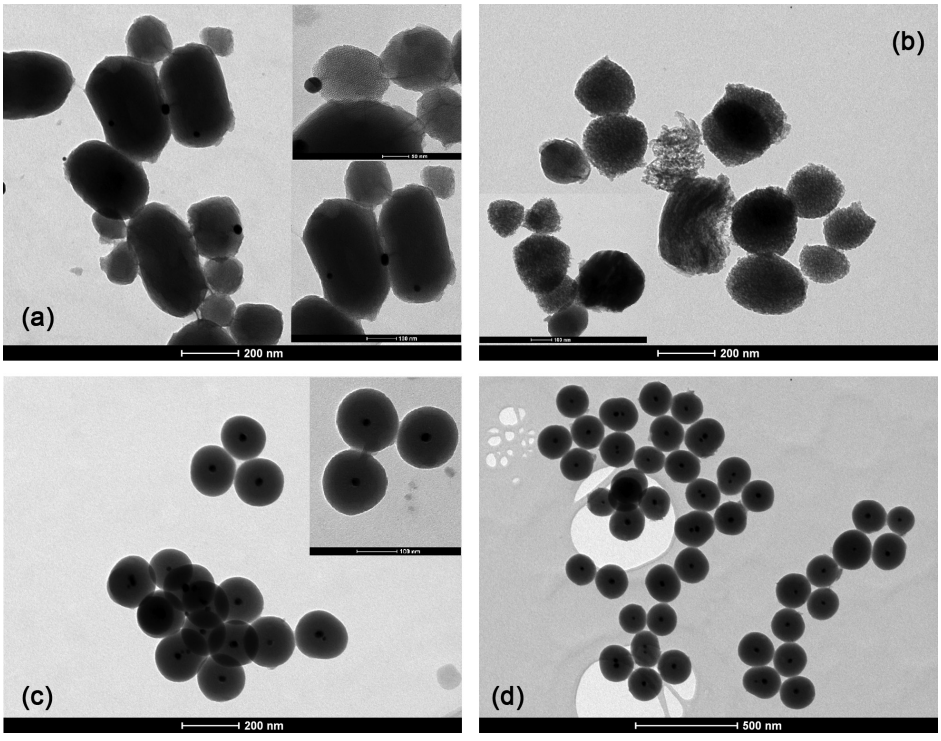

Figure 2. TEM micrographs for $AuNP/SiO_2$ before (a) and after (b) treatment with S2, and $AuNP@SiO_2$ before (c) and after (d) treatment with S2.

nanoparticles ($AuNP@SiO_2$) did not undergo structural changes after the sample treatment process, and the AuNPs are evenly distributed within the silica nanoparticles. This can be explained mainly by the fact that the silica shell in $AuNP@SiO_2$[16,17] is amorphous, with a low surface area, in contrast with the mesoporous silica used as a support in $AuNP/SiO_2$.[18,19]

Conclusions

Different sample preparation strategies for the quantification and characterization of samples with the same composition but different structural arrangements, in this case $AuNP/SiO_2$ and $AuNP@SiO_2$, were investigated. The results indicate that with the application of the S1 procedure (2 mol L^{-1} HNO_3 + 30 min stirring at 600 rpm) all of the gold added to obtain the nanoparticles was reduced ($Au^{3+} \rightarrow Au^0$). The combination of S2 (HNO_3 + HCl + MW) and S3 (HNO_3 + HCl + HF + MW) allows the presence of AuNPs on or in the silica matrix to be distinguish, i.e., the presence of supported or core-shell gold-silica nanoparticles was determined. The results are in agreement with the TEM micrographs and spectra obtained using solid-state UV-Vis spectroscopy. Moreover, based on the difference between strategies S2 and S3, it is possible to determine the gold content in or on the silica matrix present in the two types of material (silica-supported AuNPs and core-shell gold-silica NPs).

Acknowledgments

Financial support from the Brazilian research funding agencies Research and Projects Financing (FINEP), National Council of Technological and Scientific Development (CNPq), Alagoas Research Support Foundation (FAPEAL), and INCT-Catalysis are gratefully acknowledged. This study was financed in part by the Coordenação de Aperfeiçoamento de Pessoal de Nível Superior - Brasil (CAPES) - Finance Code 001. MRM and JCCS thank CNPq for the research fellowships. CJG, MJO, and ESF thank CAPES for a fellowship. Authors thank LabMET/Ufal for the transmission electron micrographs.

Author Contributions

Cristian J. Giertyas was responsible for data curation, formal analysis, investigation, methodology, writing original draft, review and editing; Victor E. S. Silva for data curation, formal analysis, investigation, and methodology; Maria J. de Oliveira for data curation, formal analysis, investigation, methodology, and writing original draft; Emerson S. Freire for data curation, formal analysis, and methodology; Josué C. C. Santos for investigation, methodology, and writing original draft, and writing review and editing; Rusiene M. de Almeida for formal analysis, methodology, supervision, and writing original draft; Mario R. Meneghetti for conceptualization, data curation, funding acquisition, investigation, methodology, project administration, resources, supervision, writing original draft, review and editing; Janaína H. Bortoluzzi for conceptualization, data curation, formal analysis, funding acquisition, investigation, methodology, project administration, resources, supervision, writing original draft, review and editing.

References

1. Li, Y.; Somorjai, G. A.; *Nano Lett.* **2010**, *10*, 2289.
2. Harding, C.; Habibpour, V.; Kunz, S.; Farnbacher, A. N.-S.; Heiz, U.; Yoon, B.; Landman, U.; *J. Am. Chem. Soc.* **2009**, *131*, 538.
3. Yeh, Y.-C.; Creran, B.; Rotello, V. M.; *Nanoscale* **2012**, *4*, 1871.
4. Gualteros, J. A. D.; Garcia, M. A. S.; da Silva, A. G. M.; Rodrigues, T. S.; Cândido, E. G.; e Silva, F. A.; Fonseca, F. C.; Quiroz, J.; de Oliveira, D. C.; de Torresi, S. I. C.; de Moura, C. V. R.; Camargo, P. H. C.; de Moura, E. M.; *J. Mater. Sci.* **2019**, *54*, 238.
5. Alshammari, A. S.; *Catalysts* **2019**, *9*, 402.
6. Cavaliere-Jaricot, S.; Darbandi, M.; Nann, T.; *Chem. Commun.* **2007**, 2031.
7. Lekeufack, D. D.; Brioude, A.; Mouti, A.; Alauzun, J. G.; Stadelmann, P.; Coleman, A. W.; Miele, P.; *Chem. Commun.* **2010**, *46*, 4544.
8. Gutiérrez, L.-F.; Hamoudi, S.; Belkacemi, K.; *Catalysts* **2011**, *1*, 97.
9. Liberman, A.; Mendez, N.; Trogler, W. C.; Kummel, A. C.; *Surf. Sci. Rep.* **2014**, *69*, 132.
10. Li, Y.; Somorjai, G. A.; *Nano Lett.* **2010**, *10*, 2289.
11. Villa, A.; Dimitratos, N.; Chan-Thaw, C. E.; Hammond, C.; Veith, G. M.; Wang, D.; Manzoli, M.; Prati, L.; Hutchings, G. J.; *Chem. Soc. Rev.* **2016**, *45*, 4953.
12. Allen, L. J.; D'Alfonso, A. J.; Freitag, B.; Klenov, D. O.; *MRS Bull.* **2012**, *37*, 47.
13. Tiruvalam, R. C.; Pritchard, J. C.; Dimitratos, N.; Lopez-Sanchez, J. A.; Edwards, J. K.; Carley, A. F.; Hutchings, G. J.; Kiely, C. J.; *Faraday Discuss.* **2011**, *152*, 63.
14. Shibata, N.; Goto, A.; Matsunaga, K.; Mizoguchi, T.; Findlay, S. D.; Yamamoto, T.; Ikuhara, Y.; *Phys. Rev. Lett.* **2009**, *102*, 136105.
15. López-Haro, M.; Cíes, J. M.; Trasobares, S.; Pérez-Omil, J. A.; Delgado, J. J.; Bernal, S.; Bayle-Guillemaud, P.; Stéphan, O.; Yoshida, K.; Boyes, E. D.; Gai, P. L.; Calvino, J. J.; *ACS Nano* **2012**, *6*, 6812.
16. Huh, S.; Wiench, J. W.; Yoo, J.-C.; Pruski, M.; Lin, V. S.-Y.; *Chem. Mater.* **2003**, *15*, 4247.

17. Trewyn, B. G.; Slowing, I. I.; Giri, S.; Chen, H.-T.; Lin, V. S.-Y.; *Acc. Chem. Res.* **2007**, *40*, 846.
18. Arnal, P. M.; Comotti, M.; Schüth, F.; *Angew. Chem., Int. Ed. Engl.* **2006**, *45*, 8224.
19. Fang, X.; Chen, C.; Liu, Z.; Liu, P.; Zheng, N.; *Nanoscale* **2011**, *3*, 1632.
20. Niemelä, M.; Pitkäaho, S.; Ojala, S.; Keiski, R. L.; Perämäki, P.; *Microchem. J.* **2012**, *101*, 75.
21. Törngren, B.; Akitsu, K.; Ylinen, A.; Sandén, S.; Jiang, H.; Ruokolainen, J.; Komatsu, M.; Hamamura, T.; Nakazaki, J.; Kubo, T.; Segawa, H.; Österbacka, R.; Smått, J.-H.; *J. Colloid Interface Sci.* **2014**, *427*, 54.
22. Kalele, S.; Gosavi, S. W.; Urban, J.; Kulkarni, S. K.; *Curr. Sci.* **2006**, *91*, 1038.
23. Tessarolli, B. O.; da Silva, P. V.; Gallardo, E. C.; Magdalena, A. G.; *Matéria (Rio de Janeiro)* **2019**, 24.

Submitted: August 24, 2021
Published online: November 22, 2021